

Time-lapse imaging and inversion of decentralized dispersed source array seismic data

Caporal, Matteo; Blacquièrè, Gerrit; Qu, Shan

DOI

[10.1190/segam2018-2995521.1](https://doi.org/10.1190/segam2018-2995521.1)

Publication date

2018

Document Version

Final published version

Published in

SEG Technical Program Expanded Abstracts 2018

Citation (APA)

Caporal, M., Blacquièrè, G., & Qu, S. (2018). Time-lapse imaging and inversion of decentralized dispersed source array seismic data. In *SEG Technical Program Expanded Abstracts 2018: 14-19 October 2018, Anaheim, United States* (pp. 221-225). (SEG Technical Program Expanded Abstracts 2018). <https://doi.org/10.1190/segam2018-2995521.1>

Important note

To cite this publication, please use the final published version (if applicable).
Please check the document version above.

Copyright

Other than for strictly personal use, it is not permitted to download, forward or distribute the text or part of it, without the consent of the author(s) and/or copyright holder(s), unless the work is under an open content license such as Creative Commons.

Takedown policy

Please contact us and provide details if you believe this document breaches copyrights.
We will remove access to the work immediately and investigate your claim.

Time-lapse imaging and inversion of decentralized Dispersed Source Array seismic data

Matteo Caporal*, Gerrit Blacquièrre and Shan Qu, Delft University of Technology

SUMMARY

In Dispersed Source Arrays (DSA) acquisitions, traditional broadband seismic sources are replaced (or supported) with dedicated narrower band devices with different central frequencies, blended together to cover the entire temporal and spatial bandwidth of interest. The recent advances in unmanned systems technology and the improved operational flexibility enabled by the limited dimensions of most DSA devices may be beneficial to the data acquisition efficiency. In fact, with DSAs the use of relatively simple autonomous devices becomes a practical proposition for seismic surveys. In a marine environment we might consider employing several autonomous source boats at the same time, while on land a combination of autonomous source trucks of varied dimensions and designs is suggested. This abstract presents a real-time decentralized and automated approach to acquisition design in order to handle the larger number of sources simultaneously operational in the field. Additionally, using the Simultaneous Joint Migration Inversion (SJMI) technology it is possible to reliably recover time-lapse information despite the significant mismatch between baseline and monitor survey geometries introduced by the decentralized acquisition method.

INTRODUCTION

The past decade has seen some substantial growth in the interest towards the Dispersed Source Arrays (DSA) acquisition method (Berkhout, 2012; Tsingas et al., 2016; Caporal et al., 2017). With this novel technology, geophysicists aim at acquiring more effectively broadband seismic data in order to improve image quality and reservoir characterization. The conventional methodology to acquire broader-bandwidth data consists of producing more energy at all frequencies utilizing broadband sources. From a practical point of view, a significant effort is required to profitably produce and operate such sources and often it is unavoidable to accept a trade-off between transmission efficiency, costs and operational flexibility. Traditional broadband sources are replaced (or supported) by several devices individually transmitting diverse and reduced frequency bands and covering together the entire bandwidth of interest. Addressing specific attention to the manufacture of different narrowband source units can drastically improve their signal emission properties and simplify their production. Furthermore, the devices dedicated to the transmission of the higher frequencies may be smaller and less powerful than conventional sources (Laws et al., 2008; Kragh et al., 2012), providing the acquisition system with increased operational flexibility. In fact, provided that the signal to noise ratio is acceptable, the required number of source units (and/or shots) producing the lower significant frequencies is relatively small. The concept received growing attention in the last years and new FWI-friendly ultralow (1-5 Hz) frequency seismic sources have already been developed both for land and offshore envi-

ronments (Reust et al. 2015, Dellinger et al. 2016).

We propose to coordinate the DSA devices simultaneously operational in the field, in a fully or semi decentralized and automated manner. In particular, every unit must be able to modify in real-time its own behavior (the moving speed and direction) in order to promptly adapt to environmental changes such as, for instance, the presence of an unexpected obstacle on its path. To do so, we chose a specific decentralized approach called *artificial potential field method* (Khatib, 1986) which proves to be particularly flexible in such situation.

In the following sections, we will first present in more detail the concepts of decentralization and artificial potential field method. Secondly, using the *Full Waveform Migration* method (FWM, Davydenko and Verschuur, 2017), a numerical example of inversion of decentralized DSA data acquired following this scheme is shown. Finally, we prove that, by choosing the *Simultaneous Joint Migration Inversion* method (SJMI, Qu and Verschuur, 2016), it is possible to efficiently deal with the significant changes in the survey geometry introduced by the non-repeatable nature of the suggested acquisition approach.

DECENTRALIZATION

Recently, decentralized system architectures inspired great advances in automation technology and new approaches to the coordination of large numbers of relatively simple devices or robots. This branch of robotics is referred to as *swarm robotics* (Bayındır and Şahin, 2007), emphasizing the analogy with natural sciences. In fact, this kind of system organization can be easily found in nature and it is commonly used, for instance, by certain insect colonies. Functions, powers and tasks are redistributed from a central location or authority and the complex behavior of the system originates in independent decisions made by lower level components operating on local information. From a practical point of view, the reliability of a swarm coordination method can be measured on the basis of three key characteristics: robustness, flexibility and scalability. Robustness can be defined as the capacity of a system to tolerate failures of single system components, flexibility is the capacity of a system to adapt to unexpected complications and dynamic environments while scalability is the ability of a system to support a smaller or larger number of individuals without appreciably impacting the overall performance.

Under this perspective, an efficient and reliable real time coordination method which is particularly suitable for the organization of DSA acquisition systems is the *artificial potential field method* (Khatib, 1986). Following this approach, each seismic source moves in a virtual field of forces influencing the target acquisition area. The position to be reached (in case there is any) is an attractive pole, while every obstacle on the field, including other source devices and optionally the target area boundaries, acts as a repulsive surface (Figure 1). The method essentially acts as a fastest descent optimization procedure forcing the source units to avoid collisions and to

remain within the boundaries of the region of interest. Outside the obstacles region of influence, the source is forced to move towards the attractive poles, for instance the recovery point or a poorly sampled area, or to move forward along its path. Artificial potential field functions can be updated with the aid of real-time data (for instance AIS and radar signals) or, when available, with the aid of more sophisticated tools aimed at improving the *situational awareness* (Endsley, 1995) of the highly dynamic acquisition systems. An excellent example of a software solution that provides a spatial and temporal overview of all simultaneous operation taking place during marine seismic acquisitions has been developed by Pember-ton et al. (2015). Geological and ecological prior information about the region of interest, from previous surveys or geological and environmental studies, may also be integrated.

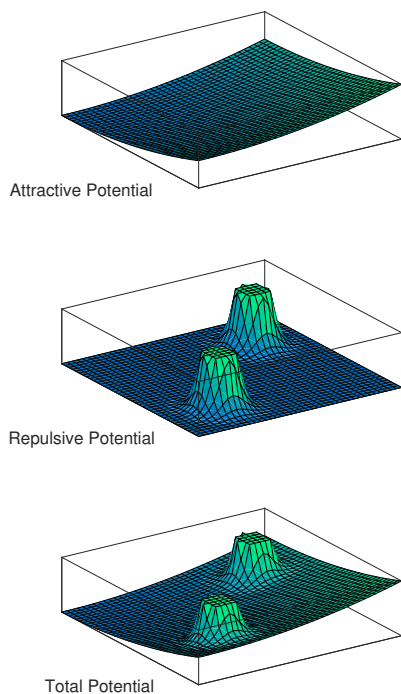


Figure 1: Example of artificial potential field functions with two obstacles and one target point (left corner).

NUMERICAL EXAMPLE: FULL WAVEFORM MIGRATION OF DECENTRALIZED DSA DATA

In this section we will present migration outputs from decentralized DSA data simulated with a real-time path coordination approach based on the artificial potential field concept. We will then compare this result with the one obtained from a centralized DSA dataset acquired on a regular shot grid.

The method utilized to perform the inversion is the so called *Full Waveform Migration* (FWM, Berkhout, 2014a; Davydenko and Verschuur, 2017). This algorithm aims at constructing the image iteratively from the reflection response, involving the exploitation of the internal and, optionally, the surface related

multiples. The inversion is driven by the residual between the modeled data (zero for the first iteration) and the measured data, which defines the update of the reflectivities for the following iterations of the algorithm. The modeled wavefield can take into account all the coda and the transmission effects, thus the observed data is explained in the correct (non-linear) way and multiple scattering contributes to the imaging, rather than compromising it. The amplitude and phase properties of the seismic data are decoupled and separately given by so called *scattering* and *propagation operators*, respectively. As a consequence, the nonlinearity in migration and inversion is decreased significantly (Berkhout, 2014a).

The numerical example is based on the 3D SEG EAGE salt model. The velocity model used as reference is shown in Figure 3a, while the density model is considered to be homogeneous. Note that the three visible sections of the velocity model shown in Figure 3a portray three orthogonal slices from inside the model. The horizontal slice (top-left) is located at $z = 750 \text{ m}$. The slice on the bottom-right is located at $x = 1000 \text{ m}$ and the slice on the bottom-left corner is located at $y = 1000 \text{ m}$. The model is 2000 m wide along both horizontal directions and 1000 m deep. Four different DSA units were considered: ultralow- ($2\text{-}6 \text{ Hz}$), low- ($5\text{-}15 \text{ Hz}$), mid- ($10\text{-}30 \text{ Hz}$) and high-frequency sources ($20\text{-}60 \text{ Hz}$). For both simulations, 8 source boats per type were deployed simultaneously except for the ultralow frequency sources, where 4 boats were deployed instead. The shot interval is irregular in order to distribute the blending noise more uniformly (between 10 m and 20 m for the high-frequency units, between 20 m and 30 m for the mid-frequency units, between 30 m and 70 m for the low-frequency units and between 50 m and 100 m for the ultralow-frequency units). The same survey duration is considered for the two experiments. For the decentralized case (Figure 2a), the sources are left free to sail within an artificial potential field generated as described in the previous section. No offline path-planning is computed beforehand. For the centralized case (Figure 2b), the source boats sail along straight lines parallel to both horizontal axes. The crossline spacing between lines is constant and equal to 100 m for the ultralow-frequency sources, 50 m for all other sources.

On the receiver side, a total of 6 floating nodes is chosen. One is placed at the center of the area of interest while the others are evenly spaced around it along a circumference of 250 m radius. Each node is positioned at a depth of 250 m below the water surface, 50 m above the ocean bottom. The receivers are recording continuously, and the result of this blended experiment is one single *supertrace* per node. The data inversion is performed without deblending (i.e., the inversion uses the 6 supertraces). All internal multiples were utilized and not removed in the inversion process.

The FWM results are presented in Figure 3b-c. The same slices as for the velocity model are portrayed. With these acquisition settings, we do not expect to properly image the whole model, especially in the larger offsets but we can see that at the final iteration the crosstalk and the blending noise are largely suppressed in both cases and the inversion results are comparable. This example proves that it is not strictly necessary to acquire data on a regular grid in order to obtain good inversion results as far as good coverage is guaranteed.

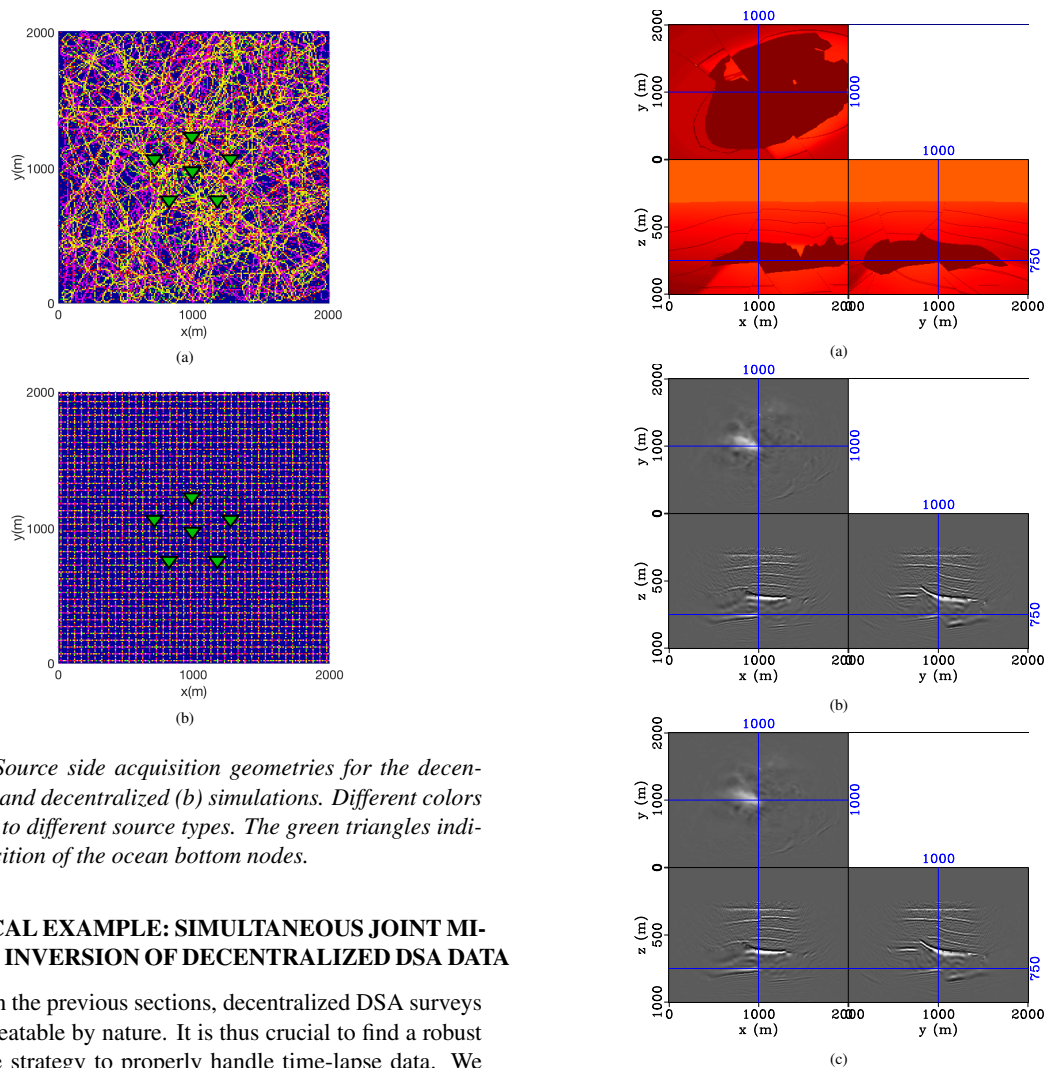


Figure 2: Source side acquisition geometries for the decentralized (a) and decentralized (b) simulations. Different colors correspond to different source types. The green triangles indicate the position of the ocean bottom nodes.

NUMERICAL EXAMPLE: SIMULTANEOUS JOINT MIGRATION INVERSION OF DECENTRALIZED DSA DATA

As shown in the previous sections, decentralized DSA surveys are non-repeatable by nature. It is thus crucial to find a robust and reliable strategy to properly handle time-lapse data. We propose a seismic monitoring method based on the so-called *Joint Migration Inversion (JMI)*, an extension of the FWM algorithm including autonomous velocity updating (Berkhout, 2014b). Being an inversion-based method, JMI does not require baseline and monitor acquisition geometries to exactly match in order to accurately estimate time-lapse perturbations, provided that the subsurface illumination is adequate (both with primary and multiples energy, Verschuur et al., 2014). Furthermore, it has been demonstrated (Wason et al., 2014; Qu and Verschuur, 2017) that time-lapse acquisition geometry changes can even provide additional information and improved monitoring results. In the light of these considerations, we propose to invert decentralized DSA time-lapse data with the so-called *Simultaneous Joint Migration Inversion (SJMI)*, Qu and Verschuur, 2016, 2017), which combines JMI with simultaneous time-lapse data processing by inverting baseline and monitor data contemporaneously.

The numerical example is based on a modified version of the well-known Marmousi model. The velocity and reflectivity models used as reference are shown in Figure 4a-b, together with the time-lapse differences (c-d). Concerning the time-lapse changes, two gas sand traps and one oil sand trap were embedded in the model. Respectively, water-gas replacements

Figure 3: Reference velocity model (a) and 3D images of decentralized (b) and centralized (c) DSA data.

modify the reservoir velocity causing an increase of 150 *m/s* while injection reduces the reservoir velocity by 200 *m/s*. Additionally, pressure perturbations and water velocity variations caused by temperature fluctuations are also considered. Internal multiple and ghost signals are not removed both in the modeling and in the inversion, see Caporal and Blacquière (2016) for a more detailed discussion on how to include them in the inversion procedure.

The inversion results of three distinct time-lapse acquisition scenarios are compared hereafter. In each case, three different source types were utilized: ultralow- (2-8 *Hz*), low- (5-20 *Hz*) and mid-frequency sources (10-40 *Hz*). In the first time-lapse acquisition scenario, repeated regular baseline and monitor survey geometries were considered. The source sampling for the ultralow-, low- and mid- frequency sources is regular and equal to 100 *m*, 40 *m* and 20 *m*, respectively. In the second and third acquisition scenarios, the acquisition geometries are non-repeated. In one case, a regular baseline

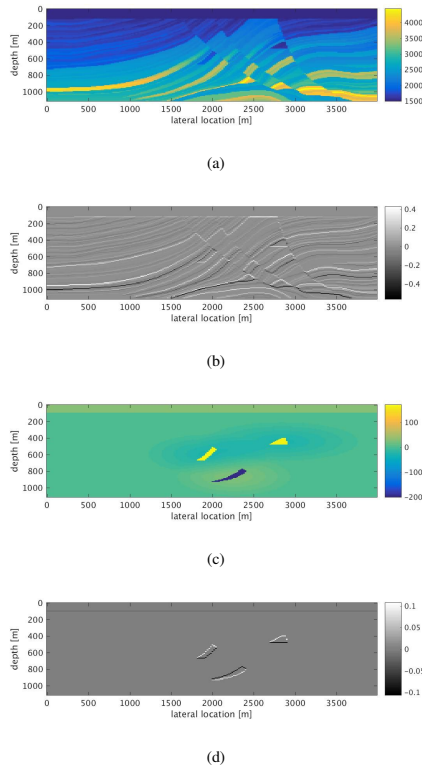


Figure 4: Reference velocity and reflectivity models for the baseline survey (a-b) and time-lapse changes (c-d).

survey is followed by a decentralized monitor survey. In the other case, both baseline and monitor surveys are decentralized (non-repeated). For the decentralized surveys, the same number of shots per source type as for the regular surveys is randomly distributed along the surface to simulate a fully decentralized acquisition. On the receiver side, the channels density and locations were not modified. The geophone interval is regular and equal to 20 m. The inverted time-lapse image and velocity for each acquisition scenario are presented in Figure 5. It is shown that SJMI can provide most time-lapse information in each case while no substantial degradation in the overall quality is introduced by the survey geometry mismatch in the decentralized acquisition scenario.

CONCLUSIONS

A major practical advantage of the Dispersed Source Array (DSA) concept is that most of its source units are smaller and less powerful than conventional sources providing the acquisition system with increased operational flexibility. To handle the larger number of sources simultaneously operational in the field, which is difficult in conventional centralized surveys, we propose to organize the acquisition system in an automated and decentralized manner. By applying this strategy it is possible to produce valid results even without path planning. A hybrid approach, which involves real-time automated path adaptations of a simple predetermined plan with the aid of live positional data, is expected to further improve this result.

Finally, using the SJMI technology it is possible to reliably recover time-lapse information even with a significant mismatch between baseline and monitor survey geometries (e.g. decentralized DSA).

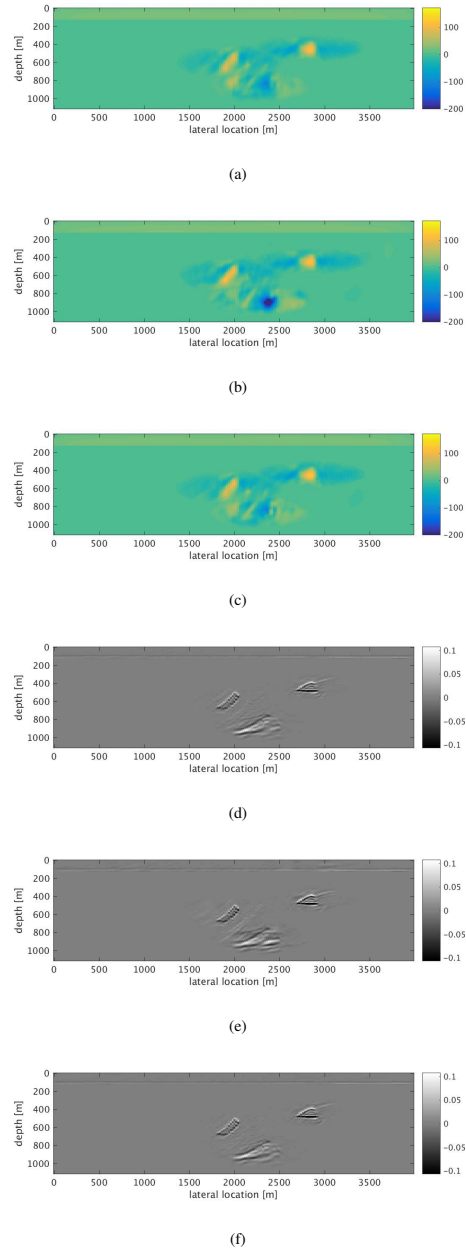


Figure 5: Inverted time-lapse results for: repeated regular baseline and monitor survey geometries (a, d), regular baseline and decentralized monitor surveys (b, e), non-matching decentralized baseline and monitor surveys (c, f).

ACKNOWLEDGEMENTS

The authors thank the sponsors of the Delphi consortium for the stimulating discussions and their financial support.

REFERENCES

- Bayindir, L., and E. Sahin, 2007, A review of studies in swarm robotics: Turkish Journal of Electrical Engineering and Computer Sciences, **15**, 115–147.
- Berkhout, A. J., 2012, Blended acquisition with dispersed source arrays: Geophysics, **77**, no. 4, A19–A23, <https://doi.org/10.1190/geo2011-0480.1>.
- Berkhout, A. J., 2014a, Review paper: An outlook on the future seismic imaging, part II: Full-wavefield migration: Geophysical Prospecting, **62**, 931–949.
- Berkhout, A. J., 2014b, Review paper: An outlook on the future seismic imaging, part III: Joint Migration Inversion: Geophysical Prospecting, **62**, 950–971.
- Caporal, M., and G. Blacquièrre, 2016, Seismic acquisition with dispersed source arrays - imaging including internal multiples and source ghost reflections: 78th Annual International Conference and Exhibition, EAGE, Extended Abstracts, <https://doi.org/10.3997/2214-4609.201600839>.
- Caporal, M., G. Blacquièrre, and M. Davydenko, 2017, Broadband imaging via direct inversion of blended dispersed source array data: Geophysical Prospecting, **66**, 942–953, <https://doi.org/10.1111/1365-2478.12584>.
- Davydenko, M., and D. J. Verschuur, 2017, Full-wavefield migration: using surface and internal multiples in imaging: Geophysical Prospecting, **65**, 7–21.
- Dellinger, J., A. Ross, D. Meaux, A. Brenders, G. Gesoff, J. T. Etgen, J. Naranjo, G. Openshaw, and M. Harper, 2016, Wolfspar, an fwi friendly ultra-low-frequency marine seismic source: 86th Ann. Internat. Mtg., Soc. Expl. Geophys., Expanded abstracts.
- Endsley, M. R., 1995, Toward a theory of situation awareness in dynamic systems: Human Factors, **37**, 32–64.
- Khatib, O., 1986, Real-time obstacle avoidance for manipulators and mobile robots: International Journal of Robotics Research, **5**, 90–98.
- Kragh, E., R. Laws, J. F. Hopperstad, and A. Kireev, 2012, Reducing the size of the seismic source with a 4C towed-marine streamer: 74th Annual International Conference and Exhibition, EAGE, Extended Abstracts, <https://doi.org/10.3997/2214-4609.20148848>.
- Laws, R. M., E. Kragh, and G. Morgan, 2008, Are seismic sources too loud?: 70th Annual International Conference and Exhibition, EAGE, Extended Abstracts, B026.
- Pemberton, G., S. Darling, C. Koehler, and E. McDonald, 2015, Managing simultaneous operations during seismic acquisition: First Break, **33**, 75–81.
- Qu, S., and D. J. Verschuur, 2016, Simultaneous time-lapse imaging via joint migration and inversion: 78th Annual International Conference and Exhibition, EAGE, Extended Abstracts, <https://doi.org/10.3997/2214-4609.201600582>.
- Qu, S., and D. J. Verschuur, 2017, Simultaneous joint migration inversion for semicontinuous time-lapse seismic data: 86th Annual International Meeting, SEG, Expanded Abstracts, 5808–5813, <https://doi.org/10.1190/segam2017-17778465.1>.
- Reust, D. K., O. A. Johnston, J. A. Giles, and S. Ballinger, 2015, Very low frequency seismic source: 85th Annual International Meeting, SEG, Expanded Abstracts, 221–225, <https://doi.org/10.1190/segam2015-5829955.1>.
- Tsingas, C., Y. S. Kim, and J. Yoo, 2016, Broadband acquisition, deblending, and imaging employing dispersed source arrays: The Leading Edge, **35**, 354–360, <https://doi.org/10.1190/tle35040354.1>.
- Verschuur, D. J., X. R. Staal, and A. J. Berkhou, 2014, Using primaries and multiples in time-lapse imaging and velocity estimation: 84th Annual International Meeting, SEG, Expanded Abstracts, 4955–4959, <https://doi.org/10.1190/segam2014-1672.1>.
- Wason, H., F. Oghenekohwo, and F. J. Herrmann, 2014, Randomization and repeatability in time-lapse marine acquisition: 84th Annual International Meeting, SEG, Expanded Abstracts, 46–51, <https://doi.org/10.1190/segam2014-1677.1>.